Title	Mathematical model of low-temperature wafer bonding under medium vacuum and its application(Published version)
Author(s)	Yu, Weibo; Wei, Jun; Tan, Cher Ming; Huang, Guang Yu
Citation	Yu, W., Wei, J., Tan, C. M., & Huang, G. Y. (2005). Mathematical model of low-temperature wafer bonding under medium vacuum and its application. IEEE Transactions on Advanced Packaging. 28(4), 650-658.
Date	2005
URL	http://hdl.handle.net/10220/5336
Rights	

Mathematical Model of Low-Temperature Wafer Bonding Under Medium Vacuum and its Application

Wei Bo Yu, Jun Wei, Cher Ming Tan, *Senior Member, IEEE*, and Guang Yu Huang

***Abstract*—Low-temperature direct wafer bonding was successfully performed under medium vacuum level. A mathematical model was developed based on the qualitative understanding of the bonding mechanisms. The model combined the diffusion-reaction model of water in SiO_2 and the diffusion theory in porous media. It is found that the model agrees well with the experimental data. This model can be applied to predict the effects of annealing time, annealing temperature, ambient vacuum, wafer orientation, and wafer dimension on the bond strength.**

***Index Terms*—Bond strength, bonding mechanisms, diffusion theory, mathematical model, wafer bonding.**

I. Introduction

DIRECT wafer bonding has attracted significant attention in the fields of microelectronics and microelectromechanical systems (MEMS). The trend now is toward low-temperature wafer bonding as traditional direct wafer bonding requires high-temperature annealing above 800 °C–1000 °C that would produce undesirable effects on the bonded materials and devices.

There are several methods to achieve high bond strength at low temperature, such as plasma-activated wafer bonding [1], nitric acid dipping wafer bonding [2], and vacuum wafer bonding. [3]–[7]. Among them, vacuum wafer bonding has the potential of becoming a reliable low-temperature bonding method.

There are several vacuum wafer bonding methods published, such as wafer bonding in ultrahigh vacuum (UHV) (10^{-10} mbar) [3], wafer bonding after Ar beam surface activation in high vacuum (10^{-8} mbar) [4], wafer bonding at medium vacuum level (10^{-4} mbar) [5], [6], and wafer bonding at low vacuum level (several mbar) [7].

In this paper, we will focus on the bonding at medium vacuum level. Although the high bond strength can be achieved with this type of bonding [5], [6], the bonding mechanisms have not been explored. It is found that the mechanisms are different from that of the traditional direct wafer bonding as well as the UHV bonding methods. On the other hand, the mechanisms exhibit similarity to low vacuum level wafer bonding to some extent.

A kinetic model for the traditional direct wafer bonding based on the interaction of water and hydroxyl groups on silica surfaces was proposed by Stengl *et al.* [8], and was further developed by Tong *et al.* to become a widely accepted wafer bonding mechanism [9]. In the model, water plays a crucial role at each stage of wafer bonding. The governing reaction is in (1). Although this model well explains the traditional wafer bonding, it cannot be applied to explain quantitatively the enhancement of bond strength in the novel low-temperature wafer bonding, such as plasma-activated wafer bonding and vacuum wafer bonding [1], [7]

$$\text{Si-O-Si} + \text{H}_2\text{O} \Leftrightarrow 2\text{Si-OH}. \tag{1}$$

As for the vacuum wafer bonding, the bonding mechanisms at different levels of vacuum are found to be distinct. For low vacuum level wafer bonding, the enhancement of the bond strength is proposed to be due to the reduction of trapped air at the bonding interface, which in turn increases the bondable area at the bonding interface and allow for the development of covalent bonds (siloxane) [7]. However, in UHV wafer bonding, two atomically clean surfaces produced in UHV make covalent bonding easier, thus attaining high bond strength [3].

As for the medium vacuum level wafer bonding, its mechanisms are rarely discussed even qualitatively [5], [6]. To our knowledge, no mathematical model has been established for the medium vacuum level wafer bonding. In this paper, we will develop a mathematical model for the medium vacuum wafer bonding by combining the diffusion–reaction theory and the theory of Knudsen diffusion in porous media. To verify our model, Si to SiO_2 direct wafer bonding was conducted at both the medium vacuum level and at air atmosphere.

II. Experiment

Bare silicon wafers and silicon wafers with thermal oxide were used in this work. The silicon wafers are standard bare CZ-grown 4-in, p-type, (100) wafers with resistivity of 1–50 Ω cm. The silicon wafers with thermal oxide of 500–600 nm thickness are also of (100) orientation. The bonding procedures were described elsewhere [5], [6]. Only Si-SiO_2 wafer bonding was performed in present work for the fabrication of SOI structure. The bond strength was measured by pull test using an Instron tensile testing machine.

In this paper, both the vacuum and air wafer bonding were performed at 200 °C, 300 °C, 400 °C, and 500°C with different annealing time of 1, 2, 3, 4, and 5 h, respectively. To obtain perfect bonding, wafers were also bonded in an oven with N_2 ambient at 800 °C for 100 h.

III. Model Development

Because the two wafers were prebonded at room temperature prior to loading into the vacuum chamber in our experiments,

Manuscript received October 25, 2004; revised March 19, 2005.

W. B. Yu, C. M. Tan, and G. Y. Huang are with the School of Electrical and Electronic Engineering, Nanyang Technological University, Singapore 639798.

J. Wei is with the Singapore Institute of Manufacturing Technology, Singapore 638075 (e-mail: jwei@simtech.a-star.edu.sg).

Digital Object Identifier 10.1109/TADVP.2005.858306

medium vacuum cannot take effect as UHV does [3]. Therefore, the mechanisms of UHV wafer bonding are not applicable in our case. Based on the mechanisms of low vacuum level wafer bonding [7], we propose that water plays a crucial role in the medium vacuum level wafer bonding and the enhancement of bond strength compared with traditional wafer bonding is due to the acceleration effect on water diffusion due to vacuum ambient.

Also, another significant basic point of our model is that the bonding interface is porous in nature right after room temperature bonding due to the surface roughness and the resulting void areas that contain neither water molecules bonded by hydrogen bonds nor Si–O–Si bonds. These void areas can be viewed as pores in the interface region called interlayer. As more bonding sites are bonded through (1), the interface gradually close up, and thus, changing the interlayer to amorphous-like SiO_2 in the annealing process. In other words, the diffusion coefficient of water along the interface will be time-dependent.

To develop a mathematical model for the mechanisms of the medium level vacuum bonding, and for the sake of simplification, we neglect the diffusion of other trapped gases, such as nitrogen, hydrogen, and so on. The justification for this assumption will be shown from the computation results shown below.

A. Identification of Diffusion Mechanism of Water

As water diffusion plays a crucial role in the bonding mechanisms, the mechanism of water diffusion in the porous interface needs to be determined. To begin, we first calculate the mean free path of water diffusion λ, which is given as follows [10]:

$$\lambda = \frac{kT}{\sqrt{2}\pi d^2 P} = \frac{kT}{\sqrt{2}\pi d^2 \frac{P_{\text{sat}}\cdot}{\text{RH}}} = \frac{1.38\times 10^{-23} * 298}{\sqrt{2}\pi \times (4\times 10^{-10})^2 \times \frac{3160}{50}} \approx 9.2\times 10^{-5}\ \text{m} \quad (2)$$

where λ is the mean free path in m, k is the Boltzmann constant, T is the absolute temperature in k, d is the diameter of water molecule, P is the partial pressure of water in Pa, P_{sat} is the saturation vapor pressure of water in Pa, and RH is the relative humidity.

From Tong's model [9], the distance between the two bonded wafers via hydrogen bonds is around 10 Å after room temperature bonding. This separation, together with the distance due to microroughness of the bonding surface that is around 5 Å on the average, the mean pore diameter can be estimated to be around 15 Å, i.e., $d_0 = 2r_0 = 1.5\times 10^{-9}$ m. This means that the pore diameter is similar to the void size in glass found in the work of Huang *et al.* [11] and Donnet *et al.* [12]. Their values are 23 and 10 Å, respectively. However, the actual average pore diameters cannot be determined directly using tunneling electron microscopy (TEM) because the bond strength after room-temperature bonding is too weak to withstand the TEM sample preparation. Also, Reznicek *et al.* performed a comparative TEM study of bonded silicon/silicon interfaces fabricated by hydrophilic [13], hydrophobic, and UHV wafer bonding, and their TEM results for hydrophilic wafer bonding at annealing temperature higher than 130 °C was found to have a pore diameter of 10 Å, and it is consistent with our estimation.

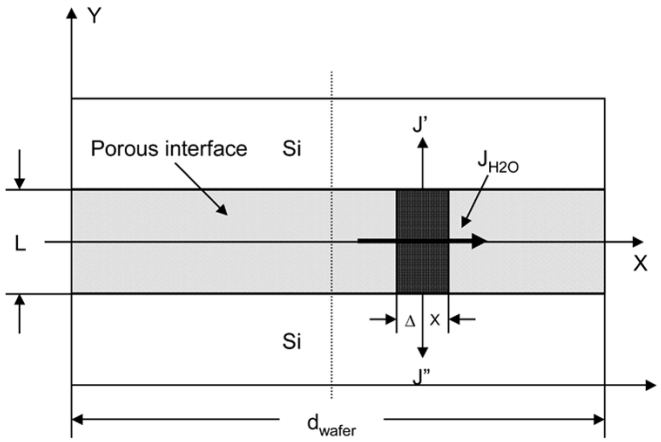

Fig. 1. Schematic of the proposed diffusion model of water at bonded interface.

With this value of average pore diameter, the Knudsen number is computed to be [14]

$$N_{Kn} = \frac{\lambda}{2r_0} = \frac{9.2\times 10^{-5}}{1.5\times 10^{-9}} = 61\,000 \gg 10. \quad (3)$$

Hence, it can be concluded that the water diffusion through the bonding interface is the Knudsen diffusion [14]. The Knudsen diffusion coefficient is independent of pressure, and it is given by [14]

$$D_K = 9700 * \bar{r}\sqrt{\frac{T}{M}} \quad (4)$$

where D_K is the diffusivity of water in cm^2/s, $\bar{r}$ is the mean radius of the pore in centimeters, T is the absolute temperature in K, and M is the molecular weight of water.

Since the interface is porous in nature as described earlier, the effective diffusivity of water needs to be modified as follows [14]:

$$D_{K,e} = D_K\frac{\varepsilon}{\tau} = 9700*\bar{r}\sqrt{\frac{T}{M}}*\frac{\varepsilon}{\tau} = 9700*\sqrt{\frac{T}{M}}*\frac{\varepsilon * \bar{r}}{\tau} \quad (5)$$

where ε is the porosity which is defined as the ratio of the unoccupied space over the total space available, and τ is the tortuosity factor of the porous interface.

B. Development of Diffusion Model

The diffusion model in this paper is shown in Fig. 1 schematically. Since the thickness of the interlayer ($L \approx$ 2–3 nm) [13] is much less than the diameter of the wafer ($d_{\text{wafer}} = 10$ cm), we can simplify this case to a one-dimensional model.

The diffusion of water out of the interlayer consists of three paths, one is the diffusion along the interface to the ambient and the other two are diffusions into the two wafers. Their respective diffusion fluxes are denoted as J_{H_2O}, J', and J'' as shown in Fig. 1. Based on the principle of mass conservation, we have

$$\begin{aligned}&(C_{H_2O,t+\Delta t} - C_{H_2O,t})_{\overline{x}} * 1 * L * \frac{\Delta x}{\Delta t}\\ &= (J_{H_2O,x,\overline{t}} * 1 * L - J_{H_2O,x+\Delta x,\overline{t}} * 1 * L)\\ &\quad + R * 1 * L * \Delta x - \left(J'_{\overline{x},\overline{t}} + J''_{\overline{x},\overline{t}}\right) * \Delta x * 1 \end{aligned} \quad (6)$$

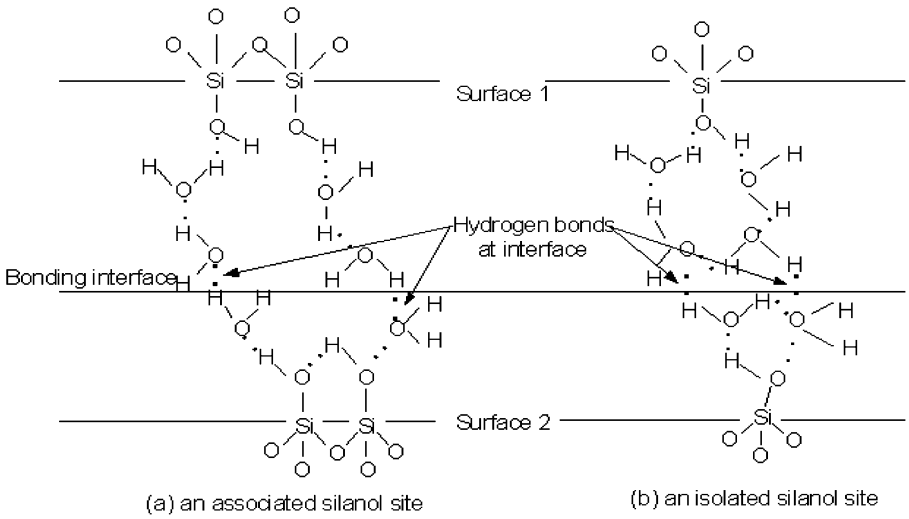

Fig. 2. Postulated interface chemical structures of hydrophilic Si/Si pairs immediately after RT contacting (a) at an associated silanol site and (b) at an isolated silanol site (reproduced from [9, Fig. 4.27] for ease of discussion).

where $C_{H_2O}(t,x)$ is the water concentration at time t and location x and R is the reaction rate of the reverse reaction of (1). Here, the width of the structure is assumed to be 1 unit.

In the case of Si-SiO_2 wafer bonding, although one Si wafer is covered by a native oxide layer, which is typically about 2–10 Å and has lower density than thermal oxide, it can not hold much of the water diffused into it, which is shown by experiments of Mack's *et al.* [15], [16]. More importantly, the water diffused through native oxide will react with the surrounding Si to form hydrogen, which will diffuse back to interface and diffuse outside along the interface. The overall number of gas molecules is not affected by this reaction, since in exchange for each consumed water molecule one hydrogen molecule is released [16]. At the condition of bonding temperature lower than 500 °C and very low water pressure, the chemical reaction of water with surrounding silicon is negligible. In the case of the thermal SiO_2-covered Si wafers, although interface water can also diffuse into the surrounding oxide, the diffusion coefficient is quite low. The time-dependent diffusion coefficients at different temperatures are calculated by Doremus's equation [17]. Comparison between vertical and transverse diffusion coefficients will be performed in the section of results and discussion, which will show that vertical diffusion coefficient is much smaller than transverse diffusion coefficient. Moreover, the vacuum effect on the diffusion of water along interface has been confirmed by experimental results of Tong *et al.*'s low vacuum wafer bonding [7] and our medium vacuum wafer bonding. Therefore, in vacuum wafer bonding, J' and J'' is negligible; thus, (6) can be simplified to

$$\begin{aligned}(C_{H_2O,t+\Delta t} - C_{H_2O,t})_{\overline{x}} * 1 * L * \frac{\Delta x}{\Delta t} \\ = (J_{H_2O,x,\overline{t}} * 1 * L - J_{H_2O,x+\Delta x,\overline{t}} * 1 * L) \\ + R * 1 * L * \Delta x. \end{aligned} \tag{7}$$

From the comparison between the bond strength of air wafer bonding and vacuum wafer bonding, it is found that vacuum bonding can improve the bond strength dramatically [5], [6]. This implies that the vacuum wafer bonding is diffusion-control process. In other words, we may presume that the reaction rate R is much faster than water diffusion during annealing.

Since there are more than one water molecules per bonding site as shown in Fig. 2, we can assume that one pair of bonding sites contact when n water molecules are diffused out, but at the same time, one water molecule is produced again according to (1). In other words, one water molecule will be produced when n water molecules diffuse out during bonding within the elemental volume shown in Fig. 1. Thus, the rate of water molecules produced by (1) is $R*1*L*\Delta x$. The rate of water diffused out of the volume is given by $(J_{H_2O,x+\Delta x,\overline{t}} - J_{H_2O,x,\overline{t}}) * 1 * L$, hence

$$\frac{R * 1 * L * \Delta x}{(J_{H_2O,x+\Delta x,\overline{t}} - J_{H_2O,x,\overline{t}}) * 1 * L} = \frac{1}{n} \equiv \delta. \tag{8}$$

Substitute (8) into (7), we have

$$\begin{aligned}(C_{H_2O,t+\Delta t} - C_{H_2O,t})_{\overline{x}} * 1 * L * \frac{\Delta x}{\Delta t} \\ = (J_{H_2O,x,\overline{t}} * 1 * L - J_{H_2O,x+\Delta x,\overline{t}} * 1 * L) \\ - \delta \bullet (J_{H_2O,x,\overline{t}} * 1 * L - J_{H_2O,x+\Delta x,\overline{t}} * 1 * L). \end{aligned} \tag{9}$$

Equation (9) may be transformed to

$$\begin{aligned}\left(\frac{C_{H_2O,t+\Delta t} - C_{H_2O,t}}{\Delta t}\right)_{\overline{x}} \\ = -(1-\delta)\left(\frac{J_{H_2O,x+\Delta x,\overline{t}} - J_{H_2O,x,\overline{t}}}{\Delta x}\right)_{\overline{t}}. \end{aligned} \tag{10}$$

Let $\Delta x \to 0$, $\Delta t \to 0$, (10) becomes

$$\frac{\partial C_{H_2O}}{\partial t} = -(1-\delta)\frac{\partial J_{H_2O}}{\partial x}. \tag{11}$$

However

$$J_{H_2O} = -D_{K,e}\frac{\partial C_{H_2O}}{\partial x}. \tag{12}$$

Hence, substitute (12) into (11), we have

$$\frac{\partial C_{H_2O}}{\partial t} = D_{K,e}(1-\delta)\frac{\partial^2 C_{H_2O}}{\partial x^2}. \tag{13}$$

Substitute (5) into (13)

$$\frac{\partial C_{H_2O}}{\partial t} = 9700 * \sqrt{\frac{T}{M}} * \frac{\varepsilon * \bar{r}}{\tau}(1-\delta)\frac{\partial^2 C_{H_2O}}{\partial x^2} = D_{\text{eff}}(t)\frac{\partial^2 C_{H_2O}}{\partial x^2} \tag{14}$$

where

$$D_{\text{eff}}(t) = 9700 * \sqrt{\frac{T}{M}} * \frac{\varepsilon * \bar{r}}{\tau}(1-\delta). \tag{15}$$

Thus, we can describe $D_{\text{eff}}(t)$ as an effective time-dependent diffusion coefficient. Intuitively, as the diffusion proceeds, ε and $\bar{r}$ decrease, τ increases, so we can assume an empirical equation for $D_{\text{eff}}(t)$ as follows:

$$D_{\text{eff}}(t) = (\eta_0 - D_{\text{equ.}})e^{-bt} + D_{\text{equ.}}. \tag{16}$$

At $t = 0$

$$\eta_0 = D_{\text{eff}}(0) = 9700 * \sqrt{\frac{T}{M}} * \frac{\varepsilon_0 * \bar{r}_0}{\tau_0}(1-\delta). \tag{17}$$

As the bonding interface becomes amorphous oxide as $t \to \infty$ [18], we can approximate $D_{\text{equ.}}$ to be the equilibrium water diffusion coefficient in silica glass [21], hence

$$D_{\text{equ.}} = 1.9 \times 10^{-4} e^{(-71/RT)} \tag{18}$$

with $D_{\text{eqn.}}$ in cm^2/s, R is the gas constant in kJ/mol $\cdot$ k, and activation energy of water diffusion is 71 kJ/mol. Then, after substituting (16) into (14), we have

$$\frac{\partial C_{H_2O}}{\partial t} = \left[(\eta_0 - D_{\text{equ.}})e^{-bt} + D_{\text{equ.}}\right]\frac{\partial^2 C_{H_2O}}{\partial x^2}. \tag{19}$$

In a heated vacuum chamber, the water concentration is extremely low, i.e., $C_{H_2O}(0,t) \approx 0$ and $C_{H_2O}(10,t) \approx 0$; hence, we have the boundary conditions as follows:

Initial Condition:

$$t = 0, \quad C_{H_2O} = C_{H_2O}(x,0). \tag{20}$$

Boundary Condition I:

$$t > 0, \quad x = 0 \text{ cm} \quad C_{H_2O}(0,t) = 0. \tag{21}$$

Boundary Condition II:

$$t > 0, \quad x = 10 \text{ cm} \quad C_{H_2O}(10,t) = 0. \tag{22}$$

C. Determination of the Bonding Strength

To determine the bonding strength, it is reasonable to assume that the strength is proportional to the concentration of chemical bonds between the two interfaces [18]. Thus, the strength can be expressed as a function of time t as follows:

$$F(t) = k_1 C_{Si\text{-}O}(t) + k_2 C_{\text{Hydro}}(t) \tag{23}$$

where $F(t)$ is the bonding strength, k_1 is the force needed to break one Si–O–Si bond, $C_{Si\text{-}O}$ is the concentration of Si–O–Si bonds between two wafers, k_2 is the force needed to break one hydrogen bond between two wafers, and $C_{\text{Hydro}}(t)$ is the concentration of the hydrogen bonds at the interface between the two wafers. For a reason that will be clear later, the relationship between $C_{\text{Hydro}}(t)$ and C_{H_2o} can be given by

$$\frac{C_{\text{Hydro}}}{C_{H_2O}} = \frac{1}{m}. \tag{24}$$

During annealing, the water is diffusing out, and, hence, the concentration of the hydrogen bonds will be decreasing and the concentration of the Si–O–Si will be increasing. If the number of total bonding sites is assumed to be constant, we have

$$C_{Si\text{-}O} = n_0 - \delta C_{H_2O} \tag{25}$$

where n_0 is the number of initially available bonding sites per unit area, which is equal to 4.6×10^{14} cm^{-2} [9], and δ accounts for the fact that there are more than one water molecule per bonding site, which has been defined in (8).

To determine the bonding strength, substitute (24) and (25) into equation (23), we have

$$F(t) = k_1 C_{Si-O} + k_2 C_{\text{Hydro}} = k_1(n_0 - \delta C_{H_2O}) + \frac{k_2}{m}C_{H_2O} = k_1 n_0 + \left(\frac{k_2}{m} - \delta k_1\right)C_{H_2O}. \tag{26}$$

Since the bond strength of the bonded pair is position-dependent over the wafer surface, the average value of the bonding strength should be used to compare with the experimental results. Hence, (26) should be written as

$$\overline{F}(t) = k_1 n_0 + \left(\frac{k_2}{3} - \delta k_1\right)\overline{C_{H_2O}(t)} \tag{27}$$

where

$$\overline{C_{H_2O}(t)} = \frac{\int_0^{d_{\text{wafer}}} C_{H_2O}(x,t)dx}{d_{\text{wafer}}}. \tag{28}$$

D. Determination of Parameters' Values

The next step is to evaluate η_0, $D_{\text{equ.}}$, b, m, k_1, and k_2. From the interface chemical structure proposed by Tong *et al.* as shown in Fig. 2, at an associated silanol site (two pairs of silanol groups), there are equivalent six water molecules as well as two effective hydrogen bonds attached, and two water molecules will be produced when this associated silanol site close and polymerize to two Si–O–Si bonds via reaction (1). For an isolated silanol site, there are six water molecules, two effective hydrogen bonds attached, and one water molecule will be produced when this site close. The results are summarized in Table I.

Since the surface density of the associated and isolated silanol groups are $C_{\text{asso}} = 3.2 \times 10^{14}$ cm^{-2} and $C_{\text{iso}} = 1.4 \times$

TABLE I
NUMBER OF FUNCTION GROUPS AT THE INTERFACE RIGHT AFTER ROOM-TEMPERATURE BONDING

Group	Number at an associated silanol site (2 pairs of silanol groups)	Number at an isolated silanol site (1 of silanol groups)
Water Molecule Attached	6	6
Effective Hydrogen	2	2
Water Molecule Produced	2	1

10^{14} cm^{-2}, respectively [9], constant "m" in (24) can be calculated as follows:

$$\begin{aligned}\frac{C_{\text{Hydro}}}{C_{H_2O}} &= \frac{1}{m} \\ &= \frac{1\times C_{\text{asso}} + 2\times C_{\text{iso}}}{\frac{6}{2}\times C_{\text{asso}} + 6\times C_{\text{iso}}} \\ &= \frac{3.2\times 10^{14} + 2\times 1.4\times 10^{14}}{3\times 3.2\times 10^{14} + 6\times 1.4\times 10^{14}} = \frac{1}{3} \end{aligned} \quad (29)$$

where the consideration is per bonding site. The initial water concentration right after room-temperature bonding at the interface can also be calculated as

$$\begin{aligned} C_{H_2O}(0) &= C_{H_2O}(x,0) = 3C_{\text{asso}} + 6C_{\text{iso}} \\ &= 3\times 3.2\times 10^{14} + 6\times 1.4\times 10^{14} \\ &= 1.8\times 10^{15}\ \text{cm}^{-2}. \end{aligned} \quad (30)$$

The value of δ can be computed according to our definition of δ as follows:

$$\begin{aligned}\delta &= \frac{1\times C_{\text{asso}} + 1\times C_{\text{iso}}}{3C_{\text{asso}} + 6C_{\text{iso}}} \\ &= \frac{n_0}{C_{H_2O}(x,0)} = \frac{4.6\times 10^{14}}{1.8\times 10^{15}} \approx 0.26. \end{aligned} \quad (31)$$

Assuming that the pores are space not covered by silanol groups and water molecules, then according to the definition of porosity as defined earlier, the initial porosity is given as

$$\varepsilon_0 = 1 - \frac{n_0}{C_{\text{Si}}} = 1 - \frac{4.6\times 10^{14}}{1.355\times 10^{15}} = 0.66 \quad (32)$$

where C_{Si} is the Si bond density on Si(100) surface [20]

$$r_0 = \frac{d_0}{2} = \frac{1.5\times 10^{-9}\ \text{nm}}{2} = 7.5\times 10^{-8}\ \text{cm}. \quad (33)$$

Assume $\tau_0 = 1.57$, (the choice of this value will be explained later), with (17) and (18), we can obtain η_0 and D_{equ} at different temperature as shown in Table II.

It is found that the bond strength of the sample saturated after 800 °C annealing without viscous flow at higher annealing temperatures, we can consider its bonding strength as $F_{\max}$. This also means that all the bonding sites have changed to Si–O–Si bonds between two wafers at this condition [9]. From our experiment results

$$F_{\max} = k_1 n_0 = 35\ \text{MPa}. \quad (34)$$

TABLE II
CONSTANTS OF (19) AT DIFFERENT TEMPERATURES

Temperature (°C)	η_0 ($\times 10^{-3}$ cm^2/s)	$D_{equ.}$ (cm^2/s)	b (s^{-1})
200	1.16	2.7×10^{-11}	3.0×10^{-4}
300	1.28	6.4×10^{-11}	1.3×10^{-4}
400	1.38	5.9×10^{-10}	5.3×10^{-5}
500	1.48	2.7×10^{-9}	3.1×10^{-5}

Then

$$k_1 = \frac{F_{\max}}{n_0}. \quad (35)$$

At $t = 0$, the bonding of the wafers is simply via the hydrogen bonding; hence

$$F_{\min} = F(0) = k_2 C_{\text{Hydro}} = \frac{k_2}{3} C_{H_2O}(0,x). \quad (36)$$

However, the bond strength at this initial condition cannot be determined as the bonded pair cannot withstand the dicing process for the sample preparation of the pull test. Instead, we can use the surface energies of the samples bonded at room temperature and 800 °C to obtain the bond strength of the sample bonded at room temperature. From Tong's model [9], surface energy at room temperature ($E_{\min}$) is 60 mJ/m^2, and surface energy at 800 °C($E_{\max}$) is 1658 mJ/m^2, thus

$$\frac{F_{\min}}{F_{\max}} = \frac{E_{\min}}{E_{\max}} = \frac{60}{1658}. \quad (37)$$

Thus

$$F_{\min} = 35 * \frac{60}{1658} = 1.27\ \text{MPa}. \quad (38)$$

Hence, from (36), we can compute the value of k_2 as

$$k_2 = \frac{3F_{\min}}{C_{H_2O}(0,x)} \quad (39)$$

and (27) can be transformed to

$$\begin{aligned}\overline{F}(t) &= k_1 n_0 + \left(\frac{k_2}{3} - \delta k_1\right)\overline{C_{H_2O}(t)} \\ &= F_{\max} + \left(\frac{\frac{3F_{\min}}{C_{H_2O}(0,x)}}{3} - \frac{n_0}{C_{H_2O}(0,x)} \bullet \frac{F_{\max}}{n_0}\right) \\ &\quad \times \overline{C_{H_2O}(t)} \\ &= F_{\max} + \frac{(F_{\min} - F_{\max})}{C_{H_2O}(0,x)} \bullet \overline{C_{H_2O}(t)} \\ &= 35 - \frac{(35 - 1.27)}{1.8\times 10^{15}} \bullet \overline{C_{H_2O}(t)} \\ &= 35 - 1.87\times 10^{-14}\overline{C_{H_2O}(t)} \end{aligned} \quad (40)$$

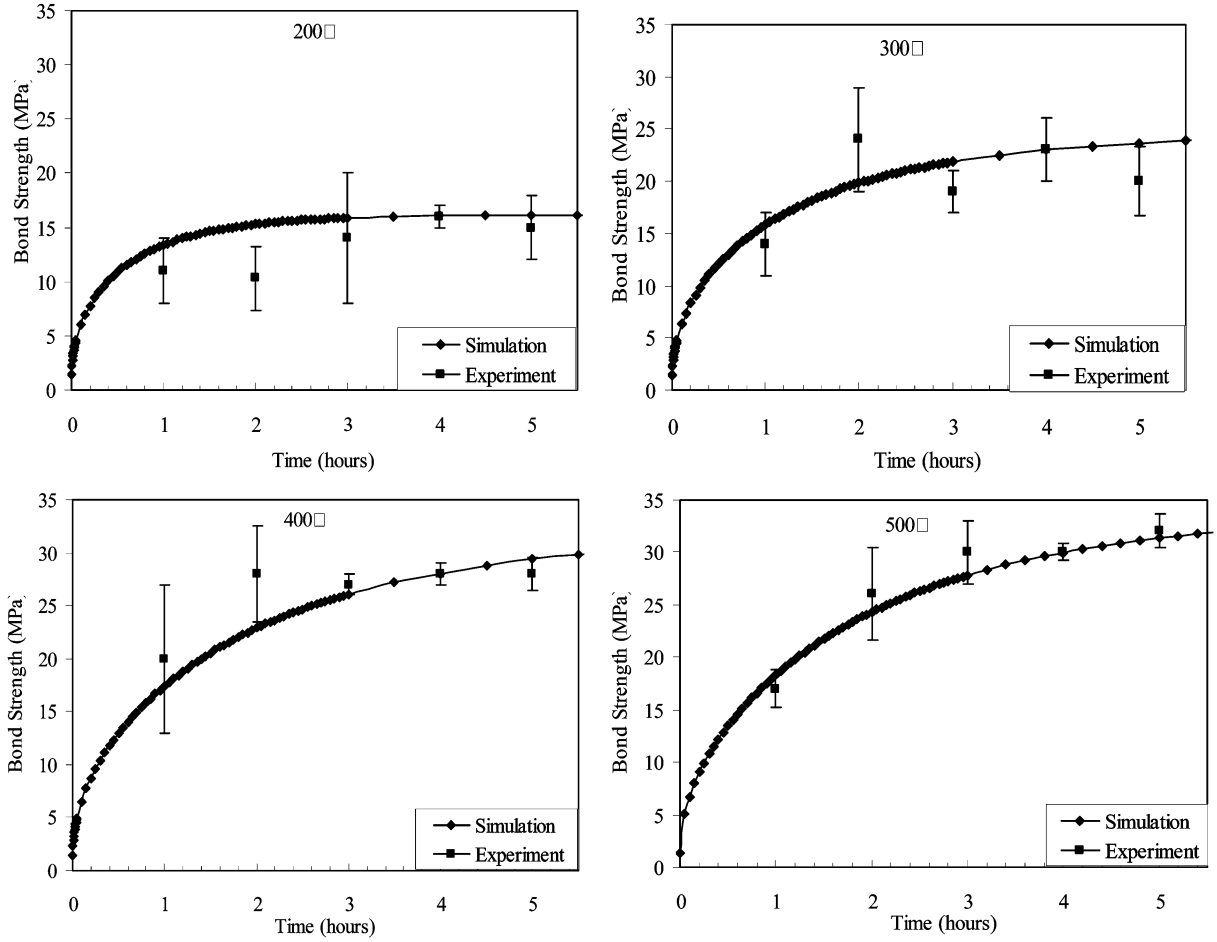

Fig. 3. Comparison between vacuum wafer bond strength of experiments and that of simulation after different annealing processes.

where F is in MPa and $\overline{C_{H_2O}(t)}$ is in cm^{-2}.

Now, let us look back at (16). The value of the constant "b" can be determined by treating it as a fitting parameter of (19) when comparing its computation results with the experimental data. The experimental data for bonding at various temperatures annealed for four hours are used for the comparison. The values of "b" is listed in Table II.

The value of the initial tortuosity factor τ_0 is set at 1.57. This is the result of many trials on the solution of the the partial differential equation (PDE) . It is found that its value has a rather limited range around 1.57. Any value of τ_0 deviates from 1.57 will render the bond strength impractical regardless of the value of "b." For smaller τ_0, the bond strength will be larger, and vice versa.

Now that the values of all the parameters needed are known, as shown in Table II, (19) can be solved using the boundary conditions in (20) to (22). Then, using (40), the change of $\bar{F}(t)$ with time can be obtained. The effect of the environment water concentration on bond strength can also be studied by changing the boundary conditions (21) and (22).

IV. Results and Discussions

This model can be applied to predict the effects of annealing time, annealing temperature, ambient vacuum, wafer orientation, and dimension on the bond strength.

A. Effect of Annealing

The simulation results of the vacuum wafer bond strength versus time at different temperatures are shown in Fig. 3. To validate our model, we superimpose the experimental results onto the simulation. It can be seen that our model agrees well with the experimental results. From this figure, the following can be made.

1) For a given annealing temperature, there is saturation for the bond strength. The higher the annealing temperature, the higher the saturated bond strength.
2) At early stage of the annealing, the rate of enhancement of the bond strength is dramatically different at different annealing temperature. Faster improvement can be seen for higher annealing temperature.
3) The saturated bond strength can be achieved in a much shorter time under medium vacuum level as compared to that of tradition wafer bonding which always takes more than 100 h [9].

B. Effect of Vacuum

The effect of vacuum can also be examined by looking at the effect of ambient water concentration (relative concentration = ambient water concentration/initial water concentration at the interface). Fig. 4 shows this effect at different annealing temperatures and different annealing time. It can be seen that the

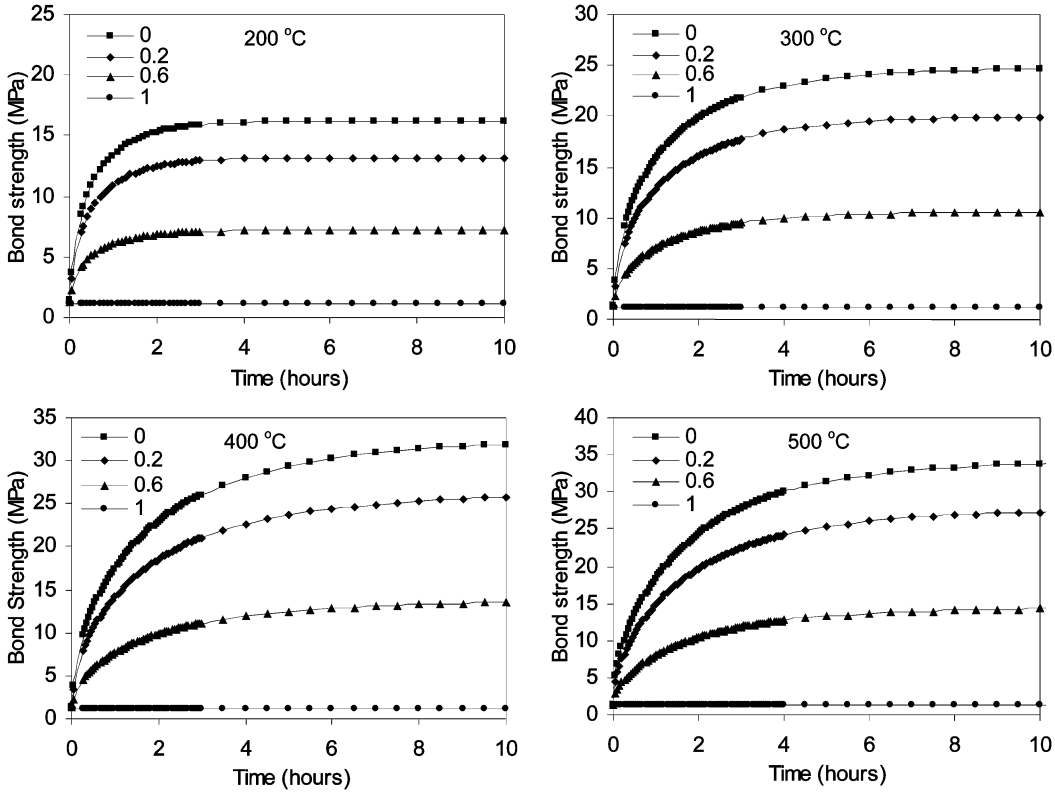

Fig. 4. Simulation results of the effect of vacuum level on bond strength.

ambient water concentration affects bond strength dramatically, and this shows the significance of vacuum level in improving the bond strength.It should be noted that in the above calculation, when the relative water concentration increases to a high value (close to 1), the model would need to be modified since vertical diffusion of water into wafers cannot be ignored.

C. Effect of Wafer Orientation

Resnik *et al.* found that wafers in the (111) orientation exhibited higher bonding abilities compared to (100) in case of bonding wafers with native oxides [19]. This was believed to be due to the higher density of available bonding sites as a consequence of enhanced chemical oxide growth rate and its homogeneity on (111) surface. In our model, the changes should be reflected on the improvement of n_0, which is the number of initially available bonding sites per unit area. Then

$$\begin{aligned}\overline{F}(t)_{(111)} &= k_1 n_{0(111)} + \left(\frac{k_2}{3} - \delta k_1\right)\overline{C_{H_2O}(t)_{(111)}} \\ &= \frac{n_{0(111)}}{n_{0(100)}} \bullet \left[F_{\max(100)} + (F_{\min(100)} - F_{\max(100)}) \right. \\ &\qquad \left. \bullet \frac{\overline{C_{H_2O}(t)_{(111)}}}{C_{H_2O}(0,x)_{(111)}}\right] \end{aligned} \tag{41}$$

where $(n_{0(111)}/n_{0(100)}) = ((1.176 \times 10^{15})/(0.677 \times 10^{15})) \approx 1.737$, available bond densities of (111) and (100) orientation are 1.176×10^{15} cm^{-2} and 0.677×10^{15} cm^{-2}, respectively [20].

The simulation results are shown in Fig. 5. It is obvious that (111)-oriented wafer bonding has higher bond strength than (100)-oriented wafer bonding which is in good agreement with the observation by Resnick *et al.* [19].

D. Effect of Wafer Dimension

Four-inch wafers are most commonly used in almost all papers published related to wafer bonding. What is the influence of dimension of as-bonded wafers on final bonding quality? The model derived in this work can predict the influence of wafer dimension on bond strength as shown in Fig. 5. From this figure, we can find that the wafer dimension has obvious influence on the bond strength: with the same annealing process, the larger the wafer, the lower the bond strength will be. It is easy to qualitatively understand this result from the basis of this model, diffusion of water trapped and produced at the interface. When the dimension is larger, the diffusion of water to ambient does need longer time. Also, more of the water will be trapped in the "dead" pore (without any channel connected to ambient) in the process of annealing. Therefore, lower bond strength is caused.

The experimental verification to study the effect of vacuum level, wafer orientation, and wafer dimension are in process now.

Finally, to further verify the simplification by ignoring the diffusion into surrounding thermal oxide, the transverse diffusion coefficients of water along the interface at different temperatures in first 5 h are shown in Table III. From Tables I and III, it can be seen that the vertical diffusion coefficients are at least 10^8 orders smaller than the transverse diffusion coefficients. Therefore, the simplification is acceptable.

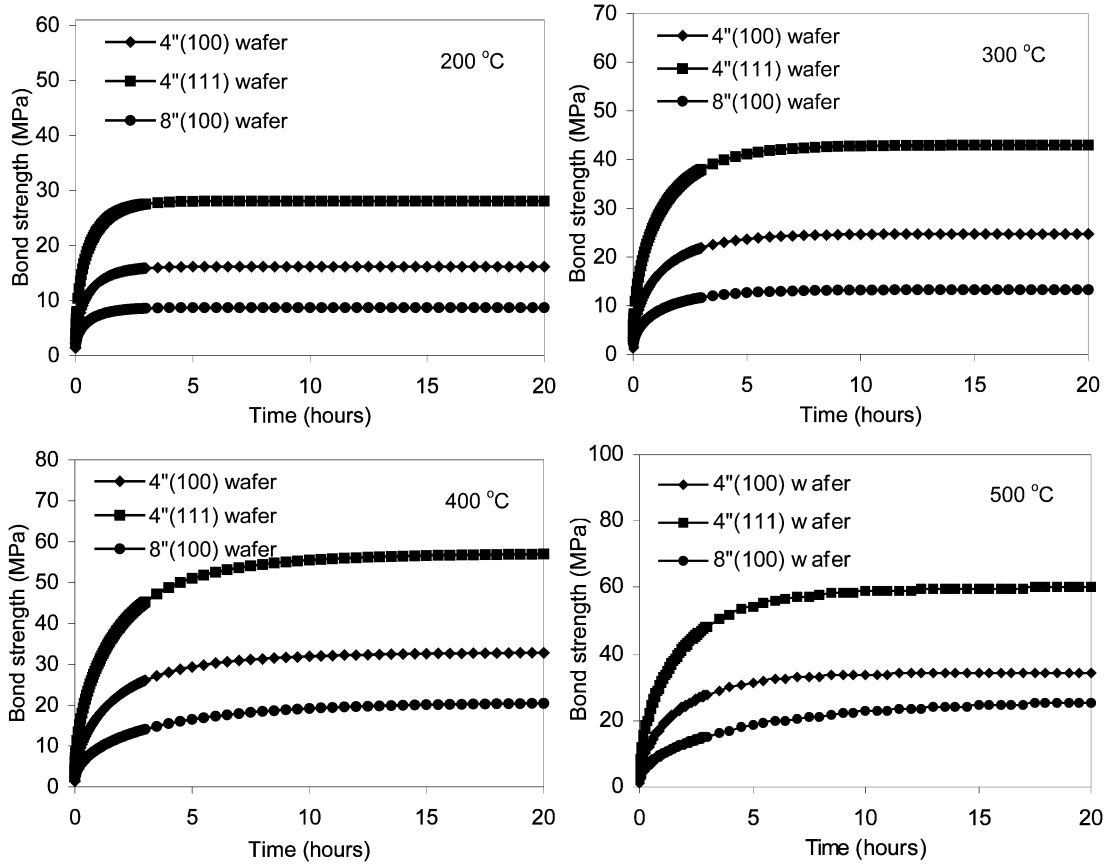

Fig. 5. Effect of wafer dimension on bond strength.

TABLE III
COMPARISON OF THE DIFFUSION COEFFICIENTS OF VERTICAL AND TRANSVERSE DIFFUSION

D (cm^2/s)		Time (hour)				
Type	**Temperature (°C)**	1	2	3	4	5
Vertical	200	7.8×10^{-11}	3.9×10^{-11}	2.6×10^{-11}	1.9×10^{-11}	1.6×10^{-11}
	300	1.4×10^{-9}	7.0×10^{-10}	4.6×10^{-10}	3.5×10^{-10}	2.8×10^{-10}
	400	1.1×10^{-8}	5.3×10^{-9}	3.5×10^{-9}	2.6×10^{-9}	2.1×10^{-9}
	500	4.7×10^{-8}	2.4×10^{-8}	1.6×10^{-8}	1.2×10^{-8}	9.5×10^{-9}
Transverse	200	0.39	0.13	4.5×10^{-2}	1.5×10^{-2}	5.2×10^{-3}
	300	0.8	0.5	0.31	0.2	0.12
	400	1.14	0.94	0.78	0.64	0.53
	500	1.32	1.18	1.06	0.95	0.85

V. CONCLUSION

Direct wafer bonding was performed under medium vacuum (10^{-4} mbar). The samples were annealed for different times at different temperatures. A mathematical model of low-temperature vacuum wafer bonding was constructed based on water diffusion and reaction, which has a crucial impact on the bond strength. The results predicted by this model agree well with the experimental results. With this model, the effects of annealing time, annealing temperature, vacuum level, wafer orientation, and wafer dimension on the bond strength are studied.

REFERENCES

[1] A. S. Velasco, P. Amirfeiz, S. Bengtsson, and C. Colinge, "Room-temperature wafer bonding using oxygen plasma treatment in reactive ion etchers with and without inductively coupled plasma," *J. Electrochem. Soc.*, vol. 150, no. 2, pp. G155–G162, 2003.

[2] A. Berthold, B. Jakoby, and M. J. Vellekoop, "Wafer-to-wafer fusion bonding of oxidized silicon to silicon at low temperatures," *Sens. Actuators A*, vol. 68, pp. 410–413, 1998.
[3] U. Gosele, H. Stenzel, T. Martini, J. Steinkirchner, D. Conrad, and K. Scheerschmidt, "Self-propagating room-temperature silicon wafer bonding in ultrahigh vacuum," *Appl. Phys. Lett.*, vol. 67, pp. 3614–3616, 1995.
[4] H. Takagi, K. Kikuchi, and R. Maeda, "Effect of surface roughness on room-temperature wafer bonding by Ar beam surface activation," *Jpn. J. Appl. Phys.*, vol. 37, pp. 4197–4203, 1998.
[5] W. B. Yu, C. M. Tan, J. Wei, S. S. Deng, and S. M. L. Nai, "Influence of applied load on vacuum wafer bonding at low temperature," *Sens. Actuators A*, vol. 115, no. 1, pp. 67–72, 2004.
[6] ——, "Influence of plasma treatment and cleaning on vacuum wafer bonding," in *Proc. IEEE Electronics Packaging Technology Conf.*, 2003, pp. 294–297.
[7] Q. Y. Tong, W. J. Kim, T. H. Lee, and U. Gosele, "Low vacuum wafer bonding," *Electrochem. Solid-State Lett.*, vol. 1, pp. 52–53, 1998.
[8] R. Stengl, T. Tan, and U. Gosele, "A model for the silicon wafer bonding process," *Jpn. J. Appl. Phys.*, vol. 28, pp. 1735–1741, 1989.
[9] Q. Y. Tong and U. Gosele, *Semiconductor Wafer Bonding: Science and Technology*. New York: Wiley, 1999.
[10] L. N. Rozanov, *Vacuum Technique*. New York: Taylor & Francis, 2002.
[11] R. J. Huang, T. Demirel, and T. D. Mcgee, "Calculation and interpretation of surface free energy of wetting of E-glass by vapors," *J. Amer. Ceram. Soc.*, vol. 56, pp. 87–91, 1973.
[12] J. B. Donnet, R. Battistella, and Chatenet, "A study of the surface of glass fibers," *Glass Technol.*, vol. 16, pp. 139–148, 1975.
[13] A. Reznicek, R. Scholz, S. Senz, and U. Gosele, "Comparative TEM study of bonded silicon/silicon interfaces fabricated by hydrophilic, hydrophobic and UHV wafer bonding," *Mater. Chem. Phys.*, vol. 81, pp. 277–280, 2003.
[14] C. J. Geankoplis, *Mass Transport Phenomena*. Ann Arbor, MI: Edwards Brothers Inc., 1982.
[15] S. Mack, H. Baumann, U. Gosele, H. Werner, and R. Schlogl, "Analysis of bonding-related gas enclosure in micromachined cavities sealed by silicon wafer bonding," *J. Electrochem. Soc.*, vol. 144, pp. 1106–1111, 1997.
[16] S. Mack, H. Baumann, and U. Gosele, "Gas development at the interface of directly bonded silicon wafers: Investigation on silicon-based pressure," *Sens. Actuators A*, vol. 56, pp. 273–277, 1996.
[17] R. H. Doremus, "Diffusion of water and oxygen in quartz: Reaction-diffusion model," *Earth Planetary Sci. Lett.*, vol. 163, pp. 43–51, 1998.
[18] B. E. Roberds, "Science and Technology of Plasma Activated Direct Wafer Bonding," Ph.D. dissertation, Dept. Elect. Comput. Eng., Univ. California, Davis, 1998.
[19] D. Resnik, D. Vrtačnik, U. Aljančič, and S. Amon, "Study of low-temperature direct bonding of (111) and (100) silicon wafers under various ambient and surface conditions," *Sens. Actuators A*, vol. 80, pp. 68–76, 2000.
[20] E. H. Nicollian and J. R. Brews, *MOS Physics and Technology*. New York: Wiley, 1982.
[21] R. H. Doremus, "Diffusion of water in crystalline and glassy oxides: Diffusion-reaction model," *J. Mater. Res.*, vol. 14, no. 9, pp. 3754–3758, 1999.

Wei Bo Yu was born in China in 1973. He received the B.Eng. and M.Eng. degrees in materials science and engineering from Zhejiang University, Hangzhou, China, in 1995 and 1998, respectively. He is currently pursuing the Ph.D. degree at Nanyang Technological University (NTU), Singapore.

He joined NTU, Singapore, as a Member of the Research Staff in 2005. His research interest is on application of wafer bonding in microelectronics, MEMS, and CNT field emission.

Jun Wei received the Ph.D. degree from Tsinghua University, Beijing, China, in 1991.

He is currently a Senior Scientist at the Singapore Institute of Manufacturing Technology, Singapore. His past R&D activities include engineering materials, coatings, and thin films. Currently, he is working on microsystems and nanosystems fabrication and packaging, low-temperature wafer/substrate bonding, advanced interconnection materials, and packaging for electronics and optoelectronics. He has published more than 150 papers in international journals and conferences. He was also invited to give the keynote address and invited speeches in many international conferences and seminars. Currently, he is serving several international conference committees.

Cher Ming Tan (SM'00) was born in Singapore in 1959. He received the B.Eng. degree (Hons) in electrical engineering from the National University of Singapore in 1984 and the M.A.Sc. and Ph.D. degrees in electrical engineering from the University of Toronto, Toronto, ON, Canada, in 1988 and 1992, respectively.

He joined the National Technological University (NTU), Singapore, as a Member of the Academic Staff in 1997, and he is now an Associate Professor in the School of Electrical and Electronic Engineering . His current research areas are mainly quality and reliability related. They are reliability data analysis, electromigration reliability physics and test methodology, and quality engineering such as QFD. He also works on silicon-on-insulator structure fabrication technology and power semiconductor device physics.

Dr. Tan is currently an Executive Committee Member of the IEEE Singapore Section, Chairman of the Certified Reliability Engineer Board for the Singapore Quality Institute, Committee Member of the Strategy and Planning Committee of the Singapore Quality Institute. He is also listed in the *Who's Who in Science and Engineering* as well as *Who's Who in the World* due to his achievement in Science and Engineering. He has also been elected to be in the Research Board of Advisors in the American Biographical Institute and the International Educator of the Year 2003 by the International Biographical Center, Cambridge, U.K. He is now appointed as the Fellow of Singapore Quality Institute, Fellow of Singapore Institute of Manufacturing Technology, and Faculty Associate of the Institute of Microelectronics.

Guang Yu Huang was born in China in 1977. He received the B.S. degree in electronic engineering from Peking University, Beijing, China, in 1999 and the M.E. degree in electronic engineering from the Graduate School of the Chinese Academy of Sciences, China, in 2002. Currently, he is a Research Assistant at the Nanyang Technological University, Singapore, working toward the Ph.D. degree.

His research interests include stress effects on partial SOI semiconductor devices.